Resonant scattering of nonlinear Schrödinger solitons from potential wells

K. T. Stoychev, M. T. Primatarowa, and R. S. Kamburova
Institute of Solid State Physics, Bulgarian Academy of Sciences, 1784 Sofia, Bulgaria
(Received 5 December 2003; revised manuscript received 23 June 2004; published 27 December 2004)

The interaction of nonlinear Schrödinger solitons with extended inhomogeneities, modeled by potential wells with different shapes, is investigated numerically. For fixed initial velocities below the transmission threshold, the scattering pattern as a function of the width of the well exhibits periodically repeating regions of trapping, transmission, and reflection. The observed effects are associated with excitation and a following resonant deexcitation (in the cases of escape) of shape oscillations of the solitons at the well boundaries. The analysis of the oscillations indicates that they are due to interference of the solitons with emitted dispersive waves.

DOI: 10.1103/PhysRevE.70.066622 PACS number(s): 05.45.Yv

Self-localized nonlinear waves (solitons) have been studied in many areas of physics, including optics, solid state, molecular, plasma, elementary particles, etc. Within integrable models, solitons exhibit remarkable stability; they propagate with constant velocities and shapes and emerge from collisions unchanged except for phase and space shifts. Real physical systems are usually described by nonintegrable equations or such containing nonintegrable perturbations. This leads to inelastic soliton interactions with a variety of outcomes. As solitons provide an important mechanism for energy and information transport in nonlinear systems, such interactions have attracted considerable attention (see, i.e., Ref. [1] for a review of earlier works on soliton dynamics in nearly integrable systems). Investigations have been focused on collisions between solitons in nonintegrable models and interactions of solitons with defects and inhomogeneities. In both cases, due to the inelasticity of the interactions, solitons can change their velocities, break into a number of localized and dispersive waves, and/or be trapped into bound states. In addition, fascinating resonance phenomena have been observed.

Resonance effects in kink-antikink collisions have been studied numerically in some nonintegrable equations including ϕ^4, double and modified sine-Gordon, and others [2–4]. For initial velocities below the threshold for trapping, a sequence of narrow regions of reflection have been obtained. These reflection windows have been explained by a "two-bounce" resonance mechanism involving excitation of an internal shape mode during the first collision, temporal trapping of the solitons due to loss of kinetic energy, deexcitation of the shape mode during the second (backward) collision, and escape of the kinks to infinity (reflection). The resonance condition requires that the time between the two collisions is commensurate with the period of the shape mode. Fine three- and four-bounce resonance structures have also been obtained [5]. Resonances in the collision of discrete NLS solitons have been investigated in [6], and in the case of vector NLS solitons-in [7].

Similar effects have been observed in the interactions of solitons with localized impurities [8–10]. It has been shown in particular that kinks can be reflected by an attractive impurity via a "two-bounce" resonance mechanism involving the excitation and deexcitation of a localized impurity modes [9], or impurity and a shape modes [10]. Scattering of nonlinear Schrödinger (NLS) solitons from point defects has been studied in [11–15] involving a variety of nonresonant outcomes.

A problem of considerable theoretical and practical importance is the interaction of solitons with extended inhomogeneities [16–18]. Nonclassical behavior in the scattering of topological solitons from potential wells has been obtained in [19–23], including a rich outcome structures of trapping, transmission and reflection as a function of the initial velocity. In the present work we investigate in detail the dynamics of NLS solitons impinging on potential wells with variable shapes. For fixed initial velocities slightly below the threshold for transmission, the increase of the width of the well yields alternating regions of capture and transmission, and, occasionally, narrow reflection windows. The regions of transmission, capture, and reflection follow a remarkable periodicity. The observed effects are explained by excitation and a following resonant deexcitation of amplitude (shape) oscillations of the soliton at the boundaries of the well.

The numerical simulations are based on the discrete nonlinear Schrödinger equation, which describes the dynamics of nonlinear Bose-type excitations in atomic and molecular chains. The potential wells are modeled by N consecutive defects, which change the local energy

$$i\frac{\partial \alpha_n}{\partial t} = -(\alpha_{n+1} + \alpha_{n-1} - 2\alpha_n) - 2|\alpha_n|^2\alpha_n + d_n\alpha_n \qquad (1)$$

$$d_n \neq 0 \text{ for } 1 \leqslant n \leqslant N, \quad d_n = 0 \text{ otherwise}.$$

In the continuum limit, (1) turns into a perturbed NLS equation

$$i\frac{\partial \alpha}{\partial t} + \frac{\partial^2 \alpha}{\partial x^2} + 2|\alpha|^2\alpha = d(x)\alpha. \qquad (2)$$

For $d(x) \equiv 0$, Eq. (2) possesses a fundamental bright soliton solution

$$\alpha(x,t) = \frac{1}{L}\,\mathrm{sech}\left(\frac{x - vt}{L}\right)e^{i(vx/2 - \omega_0 t)}, \quad \omega_0 = \frac{v^2}{4} - \frac{1}{L^2}, \quad (3)$$

where L and v are the width and the velocity, respectively, of the soliton.

It is known that for $d_n = 0$, Eq. (1) is a nonintegrable dis-

crete version of the completely integrable continuum NLS equation. For sufficiently wide solitons (compared to the lattice constant), however, the discreteness-induced effects are negligible and the solution (3) is stable on ideal discrete lattices. We checked this numerically for solitons with $L \geqslant 4$ and long time scales. So the solution (3) with $L=5.75$ was input as the initial condition in the simulations, placed 50 sites away from the defect region to avoid radiation decay due to overlapping of the soliton's tail with the potential well. A predictor-corrector method [24] was employed, periodic boundary conditions and chains much longer than the defect region in order to eliminate boundary effects. The accuracy of the calculations was controlled through the conservation of the norm (number of particles), which was better than 10^{-6} for the whole course of the simulations.

The total energy associated with the solution (3) on an ideal lattice is

$$E_s = \int_{-\infty}^{\infty} \left(\left| \frac{\partial \alpha}{\partial x} \right|^2 - |\alpha|^4 \right) dx = \frac{v^2}{2L} - \frac{2}{3L^3} \equiv E_k - E_{nl}, \quad (4)$$

where the first term describes the kinetic energy of the free quasiparticles and the second term describes the nonlinear interaction energy associated with the soliton. The scattering pattern depends, in general, on the interplay between these two energies and the energy of interaction with the defects E_d

$$E_d = \int_{-\infty}^{\infty} d(x) |\alpha|^2 dx. \quad (5)$$

The effects studied below correspond to the case of "slow solitons" with kinetic energy much smaller than the nonlinear energy $E_k \ll E_{nl}$. The large nonlinear energy is necessary in order to preserve the integrity of the soliton during the scattering.

Scattering of NLS solitons from single-point defects has been studied in detail in [11,12,14,15]. The corresponding interaction energy when the soliton is on top of the defect is

$$E_d = d \int_{-\infty}^{\infty} \delta(x) |\alpha|^2 dx = \frac{d}{L^2}. \quad (6)$$

When $E_k \gg |E_d|$, the solitons are not influenced significantly by the defect, and for $E_k \ll |E_d|$, the solitons are reflected even by an attractive defect. The possible outcomes in the case of slow solitons and moderate defect strengths ($E_k \sim |E_d|$) are transmission or capture. No resonance reflection windows have been obtained.

A natural question arises as to what happens when the defect spreads over several lattice sites. The energy of interaction with N consecutive defects when the soliton is in the middle of the defect region is

$$E_d = d \int_{-N/2}^{N/2} |\alpha|^2 dx = \frac{2d}{L} \tanh\left(\frac{N}{2L} \right). \quad (7)$$

One can expect, that for a small number of defects, ($N \leqslant L$), the evolution should be similar to this of a soliton interacting with a single defect with N-times greater strength.

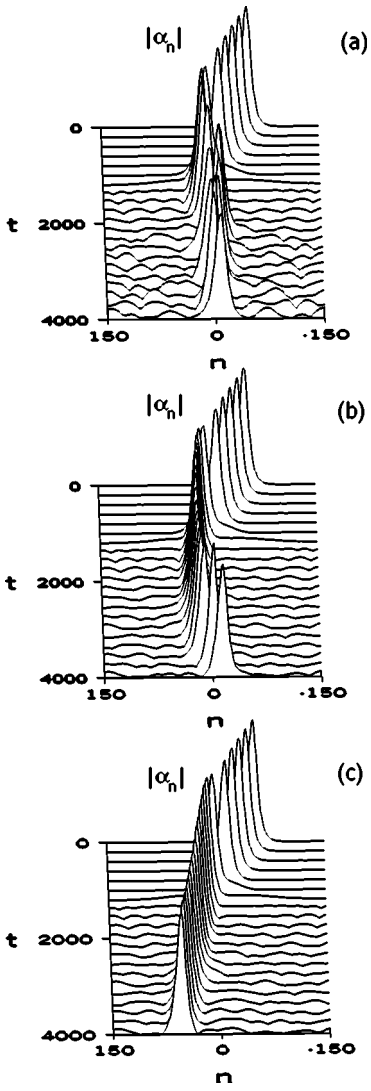

FIG. 1. Interaction of a soliton ($L=5.75$, $v=0.05$) with several consecutive impurities with a fixed summary strength. (a) $N=1$, $d=-0.035$; (b) $N=2$, $d=-0.0175$; and (c) $N=3$, $d=-0.0117$. (a) and (b) correspond to capture and (c) to transmission. The defects are centered at $n=0$.

This turns out to be true only for very small kinetic energies, when the soliton always gets trapped. For higher energies (Fig. 1), the delocalization of the defect can change the evolution from capture to transmission [Fig. 1(c)]. It is worth noting that the more localized the defect is, the stronger the radiation accompanying the interaction.

The focus of the present study lies in the interaction of NLS solitons with potential wells with variable width. The input velocity and the depth of the potential were chosen within ranges that permit a variety of scattering patterns. First we studied rectangular potential wells modeled by N consecutive defects with equal strength $d=-0.007$. The width of the wells was increased step by step to values much larger than this of the soliton. The simulations show that for initial velocities $v<0.04$ the solitons get trapped inside the well, and for $v>0.06$ they pass through it and escape to infinity for any values of N. For initial velocities in the intermediate region, the scattering pattern as a function of the

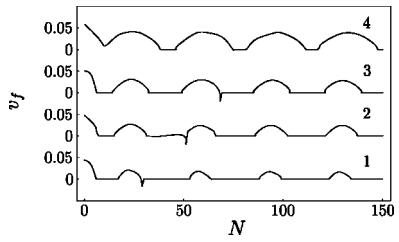

FIG. 2. Final soliton velocity v_f as a function of the number N of defects with $d=-0.007$ for different initial velocities v. Curves 1 to 4 correspond to $v=0.0440$, 0.0476, 0.0502, and 0.0580, respectively.

width of the well exhibits periodically repeating regions of transmission and capture, and occasionally, at the boundaries between them, narrow reflection windows. This is shown in Fig. 2 where we have plotted the final velocity of the soliton as a function of the width of the well for different values of the initial velocity. The horizontal parts with zero final velocity correspond to the trapping regions. The regions with positive final velocity correspond to transmission, while the narrow downward spikes with negative final velocity on curves 1–3 correspond to the reflection "windows." They are extremely sensitive to the initial velocity and difficult to observe. The relative widths of the regions of transmission and capture depend on the initial velocity and can be quite different, but the period of repeat for $N>20$ is nearly constant and depends weakly on the initial velocity.

Figures 3(a)–3(c) illustrates the evolutionary patterns corresponding to transmission, trapping, and reflection, respectively. In a trapped state [Fig. 3(b)], the soliton oscillates back and forth inside the well with zero average velocity (plotted as final on Fig. 2). In a reflection process [Fig. 3(c)],

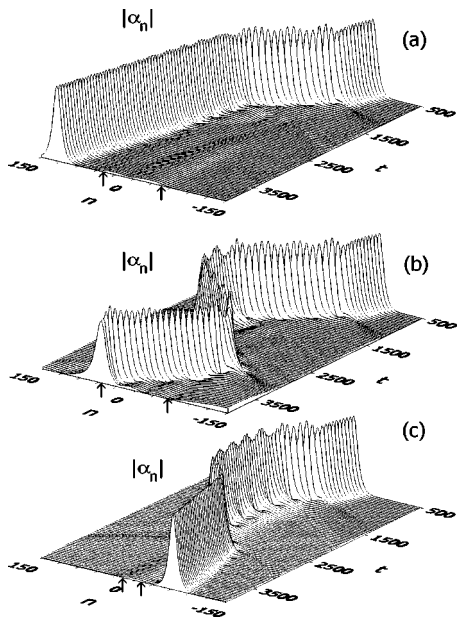

FIG. 3. Typical scattering patterns for (a) transmission ($N=95$), (b) trapping ($N=110$), and (c) reflection ($N=33$) for $v=0.05$ and $d=-0.007$. The arrows on the n-axis mark the boundaries of the defect region.

the soliton crosses the potential well, stays for a long time at the second boundary, turns back, and leaves the defect region through the first boundary. It is clearly seen that amplitude (shape) oscillations are excited when the soliton enters the potential well and persist while the soliton is inside the well. Whenever the soliton leaves the defect region, the shape oscillations are almost totally extinguished. This suggests that the shape oscillations are the cause of the periodic patterns observed on Fig. 2, and we looked for a correlation between the period of the oscillations and the width of the potential well.

The scattering patterns shown on Fig. 2 have a period of 35 (curve 1) to 36 (curve 4) lattice sites. The spatial period of the shape oscillations is not so well defined due to the variable velocity of the soliton inside the well. The temporal period of the oscillations, however, can be determined with great accuracy, and the detailed analysis of the numerical data on Fig. 3 shows that it is $T=208$. An estimate of the spatial period of the oscillations can be obtained from the following considerations: when the soliton is inside the well, its potential energy is transformed into kinetic and the soliton is accelerated. A simple energy-balance equation for this case reads

$$E_s + |E_d| = E_s', \tag{8}$$

where E_s' is the modified soliton energy. Neglecting the change of its shape and the small amount of energy taken away by the shape mode and using (4) and (7), in the case of wide potential wells ($N \gg L$, $E_d=2d/L$) we obtain

$$v^2 + 4|d| = v_1^2, \tag{9}$$

where v_1 is the modified soliton velocity inside the well. Inputting the values of v and d from Fig. 2 into (9) yields v_1 in the range 0.173–0.177. The spatial period of the corresponding oscillations is $v_1 T=36.0-36.8$. This is in excellent agreement with the period of the scattering patterns observed on Fig. 2. The values of v_1 are slightly overestimated due to the neglect of the shape oscillations in the energy balance and the reduced soliton velocity near the boundaries of the well. The broken period for narrow potential wells ($N<20$) is due to smaller interaction energy (7) in this case. The above results show that the periodic patterns of trapping, transmission, and reflection, which we observe in the scattering of NLS solitons from wide potential wells, are due to a resonance with the shape oscillations excited at the boundary.

We now address the problem of the nature of the shape oscillations. The shape oscillations in Fig. 3 have a period $T=208$ that corresponds to a frequency $\omega=-2\pi/T=-0.030$. It practically coincides with the internal frequency of the unperturbed soliton (3) $\omega_0=-0.0296$. A closer inspection of the residual oscillations of the escaping soliton shows, that they decay with time as $t^{-1/2}$. Shape oscillations of perturbed NLS solitons have been studied in [25–32]. Two main approaches have been employed for their description: (i) variational (or equivalent) and (ii) such based on the inverse scattering method [33]. The first one reduces the soliton dynamics to a set of ordinary differential equations for the pulse's parameters, while the second describes the oscilla-

tions as an interference of the soliton with the radiation accompanying the perturbed solution. The validity of the variational approach has been discussed in [30]. It has been argued that it is applicable only to solutions containing a large number of solitons, while for one-soliton solutions it can hardly be justified. In the latter case the variational approach yields oscillations with frequency $(2/\pi)\omega_0$ [26,30,31] ω_0 being the soliton frequency (3), with no radiation decay taken into account.

Dispersive perturbations of the NLS equation have been studied successfully by the inverse scattering method [25,27,28,30]. The shape oscillations obtained by this method for single-soliton solutions have a frequency of ω_0. It emerges as a beat frequency between the soliton with frequency ω_0 and dispersive waves with frequency $2\omega_0$ [28]. These modes and the corresponding shape oscillations are weakly decaying in a power law $t^{-1/2}$. The results of our numerical simulations are in excellent agreement with these based on the inverse scattering method for solitons with perturbed amplitudes. A rigorous analytical description of our results requires the solution of Zaharov-Shabat's equations [33] for a rectangular potential well, a problem that goes beyond the scope of the present paper. However, we can apply the results of [25,27,28,30] by assuming that entering the well, the soliton turns out in a different media, with a wrong amplitude. It tries to adjust to a different shape by emitting radiation. The shape oscillations on Fig. 3 are the result of the interference of the soliton with this radiation.

The periodic scattering patterns on Fig. 2 can be explained qualitatively in the following way: when the soliton reaches the potential well, it interacts inelastically with the sharp boundary and loses a small part of its kinetic energy exciting dispersive waves (radiation). Their group velocity matches the soliton velocity, and they accompany it for a long time. The interference of these waves with the soliton yields the observed oscillations of the soliton amplitude. The soliton crosses the well accompanied by the radiation, and this configuration is weakly decaying. When the soliton reaches the second boundary, different outcomes are possible, depending on the timing. In the nonresonant case, as the input initial velocities are slightly above the threshold for capture, the reduced kinetic energy of the soliton is not sufficient to overcome the potential barrier of the second boundary; the soliton is reflected from it and eventually gets trapped. However, the interaction of the oscillating soliton with the boundary is phase-sensitive and if the time for which it crosses the potential well is commensurate with the period of the shape oscillations, then the inelastic interaction with the second boundary may extinguish the shape oscillations, transferring their energy back into kinetic energy of the translational motion and allowing the soliton to overcome the barrier and escape to infinity (transmission). The higher the initial velocity of the soliton is the wider the transmission regions as seen from Fig. 2. The possible escape of a soliton from a trapped state into a propagating state due to absorption of radiation has been predicted in [22].

In some rare cases the resonant condition for escape is achieved after the soliton has crossed the defect region twice, in both the forward and backward directions. This yields the observed narrow reflection spikes in Fig. 2 corresponding to

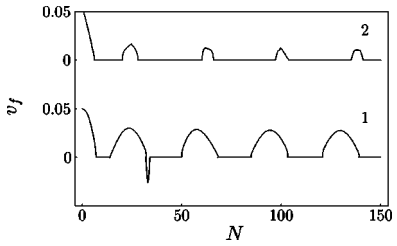

FIG. 4. Final soliton velocity v_f as a function of N for $v=0.05$ and different depths of the potential well; curve 1 corresponds to $d=-0.007$ and curve 2- to $d=-0.008$.

$v_f<0$. They are analogous to the three-bounce resonances observed in [5]. Due to the decay of the dispersive waves, these higher-order resonances are very sharp, extremely sensitive to the initial velocity, and difficult to observe. It is important to note that choosing a chain of 2000 sites and moderate time scales, we have eliminated the possibility for a spurious interaction of the soliton with radiation revolving along the chain. This was proved in a direct way by a step-by-step increase of the length of the chain, which does not change the scattering pattern.

An increase of the depth of the well leads to wider regions of trapping and narrower regions of transmission (Fig. 4, curve 2). The perturbation that the boundary induces is stronger in this case, and a larger portion of the kinetic energy of the soliton is transformed into radiation. A more exact resonance condition is required at the second boundary for the escape of the soliton, which yields narrower regions of transmission. The period of the scattering patterns in this case, determined from Fig. 4 is 38 lattice sites, while the spatial period of the corresponding shape oscillations deduced from (9) is 38.6. Again we witness an excellent agreement between the two.

Contrarily, the change of the shape of the potential well from rectangular to trapezoidal yields wider transmission regions and narrower regions of capture (Fig. 5). The potential in this case is smoother, and the perturbation it induces is weaker. Hence, a smaller portion of the kinetic energy is transformed into radiation and the resonance condition at the second boundary is more relaxed. The period of the scattering patterns does not seem to change in this case.

We also checked the dependence of the evolutionary pattern on the initial position of the soliton with respect to the boundary of the defect region. For an initial soliton in the form (3) and a fixed velocity $v=0.05$ we obtain a threshold

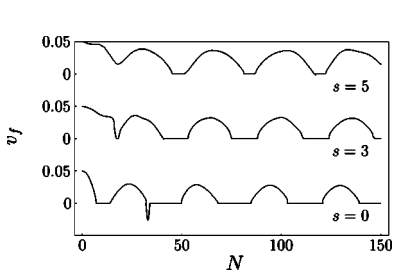

FIG. 5. Final soliton velocity v_f for $v=0.05$, $d=-0.007$ and trapezoidal potential wells with different slope (s is the extension of the slope).

initial distance of 15 lattice sites, above which the soliton passes through the defect region and below it gets trapped. This can be explained by radiation decay due to overlapping of the initial soliton with the defect region. The chaotic behavior of the outcome as a function of the initial soliton position obtained in [20] can be attributed to the different type of coupling between the soliton and the shape mode.

In summary, we have studied numerically the interaction of slow NLS solitons with extended inhomogeneities modeled by potential wells with steep boundaries and variable widths. Increasing the width of the well, we have obtained periodically repeating regions of trapping, transmission, and reflection. The observed scattering patterns are explained by an excitation and a following resonant deexcitation of shape oscillations of the solitons at the boundaries of the well. The frequency and decay analysis of these oscillations shows that they are due to interference of the solitons with small-amplitude dispersive modes (radiation), excited during their inelastic interaction with the first boundary. In the nonresonant case, due to loss of kinetic energy, the solitons get trapped inside the well. Whenever the time for which the solitons cross the well is commensurate with the period of the shape oscillations, the interaction with the second boundary may extinguish the dispersive modes, adding their energy back to the kinetic energy of the solitons and allowing the latter to escape to infinity (transmission). When the resonance condition is achieved after the solitons have crossed the well twice—in both forward and backward direction—they can escape to negative infinity, which is seen as reflection. The deexcitation of the shape oscillations at the potential boundary observed in the present numerical simulations is an interesting rare example of resonant absorption of dispersive radiation by a soliton.

ACKNOWLEDGMENT

This work is supported in part by the National Science Foundation of Bulgaria under Grant No. F911.

[1] Yu. S. Kivshar and B. A. Malomed, Rev. Mod. Phys. **61**, 763 (1989).
[2] M. J. Ablowitz, M. D. Kruskal, and J. R. Ladik, SIAM (Soc. Ind. Appl. Math.) J. Appl. Math. **36**, 478 (1979).
[3] D. K. Campbell, J. F. Schonfeld, and C. A. Wingate, Physica D **9**, 1 (1983).
[4] M. Peyrard and D. K. Campbell, Physica D **9**, 33 (1983).
[5] D. K. Campbell and M. Peyrard, Physica D **18**, 47 (1986).
[6] D. Cai, A. R. Bishop, and N. Grønbech-Jensen, Phys. Rev. E **56**, 7246 (1997).
[7] J. Yang and Yu Tan, Phys. Rev. Lett. **85**, 3624 (2000).
[8] Yu. S. Kivshar, Z. Fei, and L. Vázquez, Phys. Rev. Lett. **67**, 1177 (1991).
[9] Z. Fei, Yu. S. Kivshar, and L. Vázquez, Phys. Rev. A **45**, 6019 (1992).
[10] Z. Fei, Yu. S. Kivshar, and L. Vázquez, Phys. Rev. A **46**, 5214 (1992).
[11] Yu. S. Kivshar, A. M. Kosevich, and O. A. Chubykalo, Zh. Eksp. Teor. Fiz. **93**, 968 (1987) [Sov. Phys. JETP **66**, 545 (1987)].
[12] Yu. S. Kivshar, A. M. Kosevich, and O. A. Chubykalo, Phys. Lett. A **125**, 35 (1987).
[13] D. I. Pushkarov and R. D. Atanasov, Phys. Lett. A **149**, 287 (1990).
[14] X. D. Cao and B. A. Malomed, Phys. Lett. A **206**, 177 (1995).
[15] V. V. Konotop, D. Cai, M. Salerno, A. R. Bishop, and N. Grønbech-Jensen, Phys. Rev. E **53**, 6476 (1996).
[16] R. Sharf and A. R. Bishop, Phys. Rev. A **46**, R2973 (1992).
[17] J. J.-L. Ting and M. Peyrard, Phys. Rev. E **53**, 1011 (1996).
[18] H. Frauenkron and P. Grassberger, Phys. Rev. E **53**, 2823 (1996).
[19] G. Kälbermann, Phys. Rev. E **55**, R6360 (1997).
[20] G. Kälbermann, Phys. Lett. A **252**, 37 (1999).
[21] G. Kälbermann, Chaos, Solitons Fractals **12**, 2381 (2001).
[22] G. Kälbermann, Chaos, Solitons Fractals **12**, 625 (2001).
[23] Y. Nogami and F. M. Toyama, Phys. Lett. A **184**, 245 (1994).
[24] L. F. Shampine and M. K. Gordon, *Computer Solution of Ordinary Differential Equations* (Freeman, San Francisco, 1975).
[25] J. Satsima and N. Yajima, Suppl. Prog. Theor. Phys. **55**, 284 (1974).
[26] T. Ueda and W. L. Kath, Phys. Rev. A **42**, 563 (1990).
[27] J. P. Gordon, J. Opt. Soc. Am. B **9**, 91 (1992).
[28] M. W. Chbat, J. P. Prucnal, M. N. Islam, C. E. Soccolich, and J. P. Gordon, J. Opt. Soc. Am. B **10**, 1386 (1993).
[29] D. J. Kaup, B. A. Malomed, and R. S. Tasgal, Phys. Rev. E **48**, 3049 (1993).
[30] E. A. Kuznetsov, A. V. Mikhailov, and I. A. Shimokhin, Physica D **87**, 201 (1995).
[31] B. A. Malomed and R. S. Tasgal, Phys. Rev. E **58**, 2564 (1998).
[32] J. Yang, Phys. Rev. E **66**, 026601 (2002).
[33] V. E. Zakharov and A. B. Shabat, Zh. Eksp. Teor. Fiz. **61**, 118 (1971) [Sov. Phys. JETP **34**, 62 (1972)].